Small angle neutron scattering and gel filtration analyses of neutrophil NADPH oxidase cytosolic factors highlight the role of the C-terminal end of p47phox in the association with...

ARTICLE *in* BIOCHEMISTRY · APRIL 2001

Impact Factor: 3.02 · Source: PubMed

11 AUTHORS, INCLUDING:

Sylvestre Grizot
MedinCell
26 PUBLICATIONS **1,080** CITATIONS
SEE PROFILE

Franck Fieschi
Université Grenoble Alpes
64 PUBLICATIONS **2,419** CITATIONS
SEE PROFILE

Jean-Pierre Andrieu
Institut de Biologie Structurale (IBS)
28 PUBLICATIONS **811** CITATIONS
SEE PROFILE

Article

Small Angle Neutron Scattering and Gel Filtration Analyses of Neutrophil NADPH Oxidase Cytosolic Factors Highlight the Role of the C-Terminal End of p47[phox] in the Association with p40[phox]

S. Grizot, N. Grandvaux, F. Fieschi, J. Faur, C. Massenet, J.-P. Andrieu, A. Fuchs, P. V. Vignais, P. A. Timmins, M.-C. Dagher, and E. Pebay-Peyroula

Biochemistry, **2001**, 40 (10), 3127-3133• DOI: 10.1021/bi0028439 • Publication Date (Web): 15 February 2001

Small Angle Neutron Scattering and Gel Filtration Analyses of Neutrophil NADPH Oxidase Cytosolic Factors Highlight the Role of the C-Terminal End of p47^{phox} in the Association with p40^{phox} †

S. Grizot,[‡,§] N. Grandvaux,[§,||,⊥] F. Fieschi,[‡] J. Fauré,[||,@] C. Massenet,[‡] J.-P. Andrieu,[‡] A. Fuchs,[||] P. V. Vignais,[||] P. A. Timmins,[#] M.-C. Dagher,*[,||] and E. Pebay-Peyroula*[,‡]

Institut de Biologie Structurale, CEA-CNRS-UJF, UMR 5075, 41 rue Jules Horowitz, 38027 Grenoble Cedex 1, France, Laboratoire BBSI, CEA-CNRS-UJF, UMR 5092/Département de Biologie Moléculaire et Structurale/CEA Grenoble, 17 Rue des Martyrs, 38054 Grenoble Cedex 9, France, and Institut Laue-Langevin, 6 Rue Jules Horowitz, BP156, 38042 Grenoble Cedex 9, France

Received November 13, 2000; Revised Manuscript Received January 22, 2001

ABSTRACT: The NADPH oxidase of phagocytic cells is regulated by the cytosolic factors p47^{phox}, p67^{phox}, and p40^{phox} as well as by the Rac1−Rho-GDI heterodimer. The regulation is a consequence of protein−protein interactions involving a variety of protein domains that are well characterized in signal transduction. We have studied the behavior of the NADPH oxidase cytosolic factors in solution using small angle neutron scattering and gel filtration. p47^{phox}, two truncated forms of p47^{phox}, namely, p47^{phox} without its C-terminal end (residues 1−358) and p47^{phox} without its N-terminal end (residues 147−390), and p40^{phox} were found to be monomeric in solution. The dimeric form of p67^{phox} previously observed by gel filtration experiments was confirmed. Our small angle neutron scattering experiments show that p40^{phox} binds to the full-length p47^{phox} in solution in the absence of phosphorylation. We demonstrated that the C-terminal end of p47^{phox} is essential in this interaction. From the comparison of the presence or absence of interaction with various truncated forms of the proteins, we confirmed that the SH3 domain of p40^{phox} interacts with the C-terminal proline rich region of p47^{phox}. The radii of gyration observed for p47^{phox} and the truncated forms of p47^{phox} (without the C-terminal end or without the N-terminal end) show that all these molecules are elongated and that the N-terminal end of p47^{phox} is globular. These results suggest that the role of amphiphiles such as SDS or arachidonic acid or of p47^{phox} phosphorylation in the elicitation of NADPH oxidase activation could be to disrupt the p40^{phox}−p47^{phox} complex rather than to break an intramolecular interaction in p47^{phox}.

Neutrophils play an important role in host defense against invading microorganisms. They possess a multicomponent system, the NADPH oxidase, capable of producing superoxide anions O_2^- and other microbicidal derivatives upon activation. The superoxide-generating NADPH oxidase complex of phagocytic cells consists of a heterodimeric flavocytochrome *b*, cytosolic factors p40^{phox} (phox[1] for phagocyte oxidase), p47^{phox}, and p67^{phox}, and a small G-protein Rac1/Rac2 combined with its GDP dissociation inhibitor Rho-GDI (for reviews see refs *1* and *2*). The minimal complex which leads to the production of O_2^- ions requires the translocation of p47^{phox}, p67^{phox}, and Rac to the membrane and the association of these cytosolic factors with the flavocytochrome *b*. The translocation of the cytosolic factors is concomitant with the transient appearance of heterodimeric or heterotrimeric complexes, mediated by protein−protein interactions. The primary event for these interactions is most probably the phosphorylation of p47^{phox} which has seven phosphorylatable serine residues (*3*). Phosphorylation induces conformational changes modifying the topology of the protein and exposing domains that become accessible to specific partners (*4*). Phosphorylation also occurs on p40^{phox} and p67^{phox}, although its role is less well documented (*5*−*7*). Sequence analysis of the cytosolic factors reveals that these proteins are composed of various domains: SH3 (Src homology 3), PX (phox domain), TPR (tetratricopeptide repeat), PC (phox/Cdc42 motif), and polyPro (proline rich target) (Figure 1 and refs *8* and *9*). SH3 domains are involved in signal transduction through specific interactions with polyPro motifs. Although the presence of SH3 domains in p47^{phox}, p40^{phox}, and p67^{phox} and polyPro motifs in p47^{phox} and p67^{phox} favors such interactions, they are not the only

† The work was supported by the PCV-CNRS program, the Emergence/Region-Rhone-Alpes program, the Institut Universitaire de France, and the Direction Générale de l'Armement.

* To whom correspondence should be addressed. E-mail: pebay@ibs.fr. Telephone: 33(0)4 76 88 95 83. Fax: 33(0)4 76 88 54 94.

‡ Institut de Biologie Structurale, CEA-CNRS-UJF.

§ These authors contributed equally to this work.

|| Laboratoire BBSI, CEA-CNRS-UJF.

⊥ Present address: Molecular Oncology Group, Lady Davis Institute for Medical Research, Jewish General Hospital, 3755 chemin de la cote Sainte Catherine, H3T1E2 Montreal, Quebec, Canada.

@ Present address: Laboratoire de Biochimie, Université Sciences II, 30 quai E. Ansermet, 1211 Geneva-4, Switzerland.

Institut Laue-Langevin.

[1] Abbreviations: phox, phagocyte oxidase; SH3, Src homology 3; PX, PhoX domain (present in the N-terminal region of p47^{phox} and p40^{phox}); TPR, tetratricopeptide repeat; PC, phox/Cdc24p motif (present in p40^{phox} and Cdc24p); polyPro, proline rich target; Trx, thioredoxin; SANS, small angle neutron scattering; MBP, maltose binding protein.

10.1021/bi0028439 CCC: $20.00
Published on Web 02/15/2001

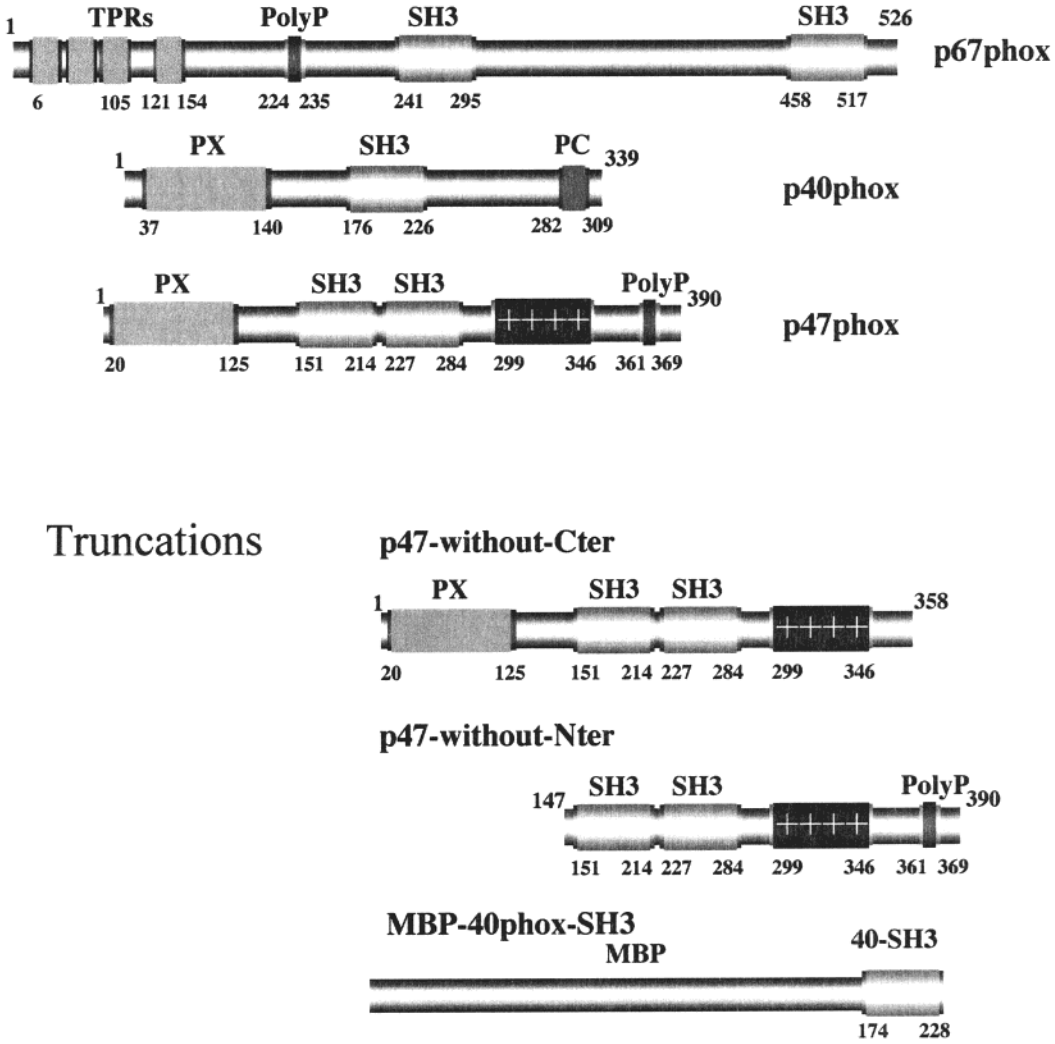

FIGURE 1: Schematic representation of the cytosolic factors and their domains. The figure depicts various proteins and their truncated forms described in the text and highlights the SH3, PX, PC, polyPro, and TPR domains. For MBP-SH3^{p40phox}, the residues are numbered according to the sequence of p40^{phox}.

sequences that may account for the formation of transient associations between proteins. In particular, p40^{phox} interacts with p67^{phox} through a PC sequence rich in acidic amino acids at the C-terminus (*8*, *9*). In addition, interaction between Rac and p67^{phox} (*10*−*12*) appears to involve specific sequences at the N-terminal end of p67^{phox}, and it was postulated that the Rac1−p67^{phox} complex might influence the binding of p67^{phox} to p47^{phox} (*13*).

Interactions between isolated domains in proteins are not easily identified in vitro as they generally display rather low binding affinities ($K_d = 5-100$ μM). However, the interactions that they mediate may be strengthened by the presence of surrounding residues by several orders of magnitude (*14*, *15*). Therefore, full-length proteins and only partially truncated proteins are, by far, the most appropriate materials for the study of protein complexes. Protein interactions are generally studied using in vitro binding assays on protein domains bound to beads. Small angle neutron scattering (SANS) experiments in solution give access to both the molecular mass and thus the oligomerization state of the molecules and their radius of gyration and thus the shape of the molecules. Additionally, SANS is particularly adapted to studying complexes with high K_d values as the measurement is taken on a solution in which the complex is in equilibrium with its components in contrast to a gel filtration experiment. In this paper, by combining a biophysical and biochemical approach, small angle neutron scattering and gel filtration, we demonstrate the existence of the monomeric state of p40^{phox}, of p47^{phox}, and also of partially truncated forms of p47^{phox}, namely, p47^{phox}-without-Nter and p47^{phox}-without-Cter, and the dimeric state of p67^{phox}. We also show that p47^{phox} forms a 1:1 complex with p40^{phox} which requires the C-terminal end of p47^{phox}.

EXPERIMENTAL PROCEDURES

Biochemical and Molecular Biology Reagents

Kits for plasmid preparation, PCR, and excised DNA fragment purification are from QIAGEN. Oligonucleotides used for PCR are from Eurogentec. Restriction enzymes are from Roche. The polymerase used in PCR amplification is the Pfu polymerase from Stratagene. DNA sequencing was carried out by Genome Express (Grenoble, France). All other reagents are from Sigma Chemicals.

Sample Preparation

p40^{phox}. Cloning of p40^{phox} cDNA into the pET32a(+) vector (Novagen) downstream of the thioredoxin (Trx) and

His_6 tag coding sequences and overexpression of Trx-His-p40^{phox} in *Escherichia coli* BL21(DE3) cells were performed as described previously (*16*). Trx-His-p40^{phox} was isolated by affinity chromatography through loading of the bacterial lysate at a rate of 1 mL/min on 1.5 mL of Ni^{2+}-charged beads (Probond, Invitrogen) packed in an FPLC column and equilibrated in 20 mM Hepes (pH 7.9) and 0.5 M NaCl supplemented with 10 mM imidazole. Proteins were eluted with a 30 mL linear imidazole gradient (from 10 to 200 mM) at a rate of 1 mL/min. Fractions containing Trx-His-p40^{phox} were pooled and subjected to overnight digestion at 4 °C with 20 units of enterokinase/mg of fusion protein in the presence of 1 mM $CaCl_2$ and 0.1% Tween 20. Digestion products were separated by a 1 h incubation with Ni^{2+}-charged beads at 4 °C. The digested recombinant protein, p40^{phox}, present in the bead supernatant was further purified by chromatography on a MonoS Fast Flow column (HR5/5, Pharmacia) equilibrated in 20 mM Hepes (pH 7.9). Proteins were eluted with a 30 mL linear NaCl gradient (from 150 to 500 mM) at a rate of 0.5 mL/min.

p47^{phox}-without-Cter. An *Xba*I fragment containing the full-length p47^{phox} sequence (*17*) was subcloned into the pAlter 1 vector (Promega). The fragment was excised using *Eco*RI and *Sal*I and subcloned into pGEX4T2 (Pharmacia). The protein was overexpressed as described for p40^{phox}, purified on glutathione−Sepharose beads (Pharmacia), and cleaved by thrombin (Sigma) overnight at 4 °C using 1 unit of thrombin/L of culture. The bead supernatant was then diluted in 50 mM Mes (pH 6.5), 1 mM EGTA, and 200 μM DTT, and p47^{phox} was further purified on a Mono S HR5/5 column (Pharmacia). The protein was eluted with 450 mM ammonium acetate in the same buffer. Thrombin cleavage induced a truncation of the C-terminus of p47^{phox} after R358 as determined by mass spectroscopy and N-terminal sequencing.

p47^{phox}-without-Nter. The cDNA for p47^{phox}-without-Nter (amino acid residues 147−390) was constructed by PCR using specific primers, cloned into pET-30b (Novagen), and checked by sequencing. The protein was overexpressed as described for p40^{phox}. The bacterial pellet was resuspended in 20 mM Hepes (pH 7.5), 250 mM NaCl, 20 mM imidazole, and 10 μg/mL leupeptin. After disruption of the cells by sonication, the lysate was injected onto Ni^{2+}-charged beads packed in an FPLC column and equilibrated in 20 mM Hepes (pH 7.5) and 250 mM NaCl. Proteins were eluted with a 60 mL linear gradient of imidazole (from 0 to 300 mM) at a rate of 1 mL/min. Fractions containing p47^{phox}-without-Nter were pooled and loaded on a column packed with SP-Sepharose beads (Pharmacia) equilibrated in 20 mM Hepes (pH 7.5). The elution was performed with a 30 mL linear gradient of NaCl (from 0 to 500 mM) at a rate of 0.5 mL/min. The protein was then concentrated to 3 mL and loaded at a rate of 1 mL/min onto the Hiload 16/60 Superdex 200 gel filtration column (Pharmacia) equilibrated in 20 mM Hepes (pH 7.5), 150 mM NaCl, and 5 mM DTT.

p47^{phox}. The cDNA fragment encoding full-length p47^{phox} was obtained by PCR, cloned into pET-15b (Novagen), and checked by sequencing. Overexpression was performed as described for p40^{phox}. The first step of the purification was carried out using Ni^{2+}-charged beads by following the same protocol that was used for p47^{phox}-without-Nter. At this stage, there were two forms of p47^{phox}. N-Terminal sequencing and mass spectrometry experiments showed that the full-length protein coexisted with a truncated form most probably cleaved after R354, very similar to p47^{phox}-without-Cter. The two proteins were loaded onto a Mono S HR 5/5 column (Pharmacia) equilibrated in 20 mM Hepes (pH 7.5). An elution with a 50 mL linear NaCl gradient (from 0 to 500 mM at a rate of 0.5 mL/min) allowed the isolation of the full-length p47^{phox} in the last fractions of the elution peak.

MBP-SH3^{p40phox}. A cDNA fragment encoding the p40^{phox} SH3 module, from R174 to K228, was amplified by PCR using the full-length p40^{phox} sequence (*18*) as a template. The PCR fragment was cloned into the pCRscript Amp SK(+) cloning vector according to the manufacturer's protocol (Stratagene). The resulting pCRscript-SH3^{p40phox} plasmid was cleaved with *Kpn*I and *Xba*I, and the 168-base fragment containing the SH3^{p40phox} sequence was subcloned in pMAL-C2E (New England Biolabs). The resulting vector named pMal-SH3^{p40phox} was transformed and amplified in DH5α. The sequence of the construct was checked. The MBP-SH3^{p40phox} was overexpressed as described for p40^{phox}. After 3 h, cells were harvested and resuspended in chilled lysis buffer [20 mM Hepes (pH 7.5) and 150 mM NaCl]. All of the following operations were carried out at 4 °C. Cells were disrupted by sonication. After centrifugation at 40 000 rpm for 40 min in a Beckman 45 Ti rotor, the supernatant was loaded at a rate of 0.7 mL/min onto 20 mL of amylose resin (New England Biolabs) packed in an FPLC column previously equilibrated with 20 mM Hepes (pH 7.5) and 150 mM NaCl. The column was washed with 5 column volumes of buffer, and bound proteins were eluted with the same buffer supplemented with 20 mM maltose. The resulting protein fractions containing MBP-SH3^{p40phox} were pooled and diluted to decrease the concentration of NaCl to 50 mM and then loaded onto a 5 mL High Q column (Bio-Rad) equilibrated with 20 mM Hepes (pH 7.5). The column was washed, and the MBP-SH3^{p40phox} fusion protein was eluted with the same buffer containing 100 mM NaCl. MBP-SH3^{p40phox} was concentrated to 30 mg/mL.

Formation of the Complex of MBP-SH3^{p40phox} with p47^{phox}-without-Nter. MBP-SH3^{p40phox} and p47^{phox}-without-Nter were mixed at a 1:1 stoichiometry. The mixed solution was loaded onto an amylose column (1 mL) equilibrated with 20 mM Hepes (pH 7.5), 150 mM NaCl, and 5 mM DTT. After washing, proteins were eluted with the same buffer supplemented with 20 mM maltose. Fractions containing both MBP-SH3^{p40phox} and p47^{phox}-without-Nter, as determined by SDS−PAGE analysis, were pooled and concentrated.

p67^{phox}. p67^{phox} cDNA was cloned from a dibutyryl AMPc differentiated HL60 cell cDNA library as described previously (*17*). A *Pst*I−*Hin*dIII fragment containing the full-length cDNA was subcloned into the pBluebac His A vector (Invitrogen) in frame with the N-terminal polyhistidine sequence. A recombinant baculovirus was made using classical protocols. For expression of the protein, high-titer virus stocks were used to infect insect cells at a density of 2×10^6 cells/mL with a multiplicity of infection of 5. Cells were collected 48 h postinfection. The cell pellet was washed in PBS and resuspended in 5 pellet volumes of 10 mM Hepes (pH 7.5), 50 mM NaCl, and 100 μM DTT supplemented with the following protease inhibitors, 1 mM DFP and 10 μg/mL leupeptin. The cells were disrupted by sonication. The lysate was mixed with an equal volume of the same

buffer containing glycerol and NaCl to final glycerol and NaCl concentrations of 17% and 0.5 M, respectively, and centrifuged at 300000*g* for 45 min at 4 °C. $p67^{phox}$ was purified from the high-speed supernatant by incubation for 1 h at 4 °C with 1 mL of Ni^{2+}-charged beads with gentle rotation. The beads were then packed onto an FPLC HR 5/5 column, washed with the same buffer containing 10 mM imidazole, and eluted with 200 mM imidazole.

All proteins were concentrated on Amicon membranes. Pure protein yields were 0.3, 0.2, 3, 1, 5, and 0.5 mg/L of culture for $p40^{phox}$, $p47^{phox}$-without-Cter, $p47^{phox}$-without-Nter, $p47^{phox}$, MBP-$SH3^{p40phox}$, and $p67^{phox}$, respectively. Their homogeneity was checked by SDS−PAGE.

Small Angle Neutron Scattering

The neutron scattering was performed at Institut Laue-Langevin on beamlines D11 (*19*) and D22. The samples were contained in 1 mm path length quartz cuvettes (Hellma, France) containing 150 μL of protein solution. Scattered intensities were recorded using a two-dimensional detector. The wavelength was set to 10 Å and the detector placed 3 or 6 m from the sample on D11 or D22, respectively. The samples were maintained at 4 °C during the data collection by circulating water around the sample holder. Scattering from each sample was measured for approximately 1−2 h to obtain a correct signal-to-noise ratio. All the samples were assessed in H_2O buffer.

Data Reduction and Analysis

Scattered intensities from protein solutions, buffers, water, and an empty cell were recorded using a two-dimensional detector, and summed radially (*20*). The scattered intensities from the proteins, $I(q)$, were obtained by correcting for the contribution of the buffer and cell and the nonuniformity of the detector response, using the following expression:

$$I(q) = [I_s(q) - T_s I_{buf}(q)]/[I_w(q) - T_w I_{ec}(q)]$$

where $I_s(q)$, $I_{buf}(q)$, $I_w(q)$, and $I_{ec}(q)$ are the scattered intensities from the sample, the buffer, the water, and the empty cell, respectively, T_s and T_w are the transmissions of sample and water, respectively, and q is the amplitude of the scattering vector related to the scattering angle 2θ and to the wavelength λ by the relation $q = 4\pi \sin \theta/\lambda$. This procedure also puts all data together on the same relative scale (i.e., normalized to the scattering of water). The data can then be related to absolute molecular weigths by the procedure of Jacrot and Zaccai (*21*) as described below. In the low-q region, the scattered intensity from monodisperse solutions can be approximated by Guinier's law:

$$\ln[I(q)] = \ln[I(0)] - {}^1/_3 R_g{}^2 q^2$$

The linearity of the Guinier plots, $\ln[I(q)]$ versus q^2, in the low-q region allowed us to check for a nonaggregated state of the molecules. The zero-angle scattering intensity, $I(0)$, and the radius of gyration, R_g, were derived by a least-squares method from the Guinier plots. The molecular mass M of the molecules in solution is derived from $I(0)$ by the relation $I(0) = kcM$, where c is the protein concentration in milligrams per milliliter and k is a factor expressed in milliliter per milligram per dalton:

$$k = [4\pi T_s t f N_A (\sum b/M - \rho_s V/M)^2]/(1 - T_w)$$

where T_s and T_w are the transmissions of the sample and water, respectively, t is the thickness of the sample in centimeters (0.1 cm), f is a wavelength-dependent correction factor equal to 1 for $\lambda = 10$ Å, N_A is Avogadro's number, $\Sigma b/M$ is the sum of scattering lengths per unit of molecular mass, ρ_s is the scattering length density of the solvent (-0.56×10^{10} cm^{-2} for H_2O), and V/M is the molecular volume per unit molecular mass. V/M is also equal to υ/N_A, υ being the partial specific volume (0.745 cm^3/g). $\Sigma b/M$ was computed for each protein, taking into account its amino acid composition. The normalization of $I(0)$ and the derivation of the molecular mass are described in more detail elsewhere (*21*, *22*).

Gel Filtration Analysis

The Superdex 200 gel filtration column (Pharmacia) was equilibrated in 20 mM Hepes (pH 7.5) and 150 mM NaCl supplemented with 5 mM DTT for the MBP-$SH3^{p40phox}$—$p47^{phox}$-without-Nter complex. Samples were concentrated to 0.2−0.5 mL and loaded onto the columns at a flow rate of 0.5 mL/min. Protein elution was pursued at 0.5 mL/min and monitored by recording the absorbance at 280 nm. For calibration, the following molecular mass markers were used: IgG (150 kDa), bovine serum albumin (67 kDa), ovalbumin (43 kDa), and cytochrome *c* (14 kDa).

Concentration Determination by Amino Acid Assessment

The concentrations of protein samples were determined by quantitative amino acid analysis (*23*). Samples were dried and hydrolyzed at 110 °C in constant-boiling HCl containing 1% (v/v) phenol, for 24 h under reduced pressure and in the absence of oxygen. Amino acids were analyzed on a model 7300 Beckman amino acid analyzer, with the standard sodium citrate eluting buffer system. Calibrations were made with aliquots of three to five standard solutions, each of which contained all the amino acids except tryptophan. For some samples, norleucine was added as an internal standard prior to lyophilization. All amino acids, except Trp, Cys, and Met for $p47^{phox}$ and $p67^{phox}$ and Trp, Cys, Met, Thr, and Ala for $p40^{phox}$, were used to determine the concentrations. Each sample was divided into at least two aliquots for the amino acid analysis. The concentrations obtained in each aliquot are identical, and the deviations between the experimental and theoretical amino acid compositions are within a few percent.

RESULTS

Small Angle Neutron Scattering

Figure 1 shows schematically the whole cytosolic phox proteins and their truncated forms used in our experiments. It highlights the domains and motifs present in each protein. The solubility of the proteins was examined first. Preliminary experiments revealed the poor solubility of $p47^{phox}$, $p40^{phox}$, and $p67^{phox}$, for which the maximum concentrations without aggregation are ~5, ~2, and ~1 mg/mL, respectively. To overcome the heterogeneity in shape and association resulting from phosphorylation, we first chose to study the nonphosphorylated proteins $p47^{phox}$ and $p40^{phox}$ expressed in bacteria.

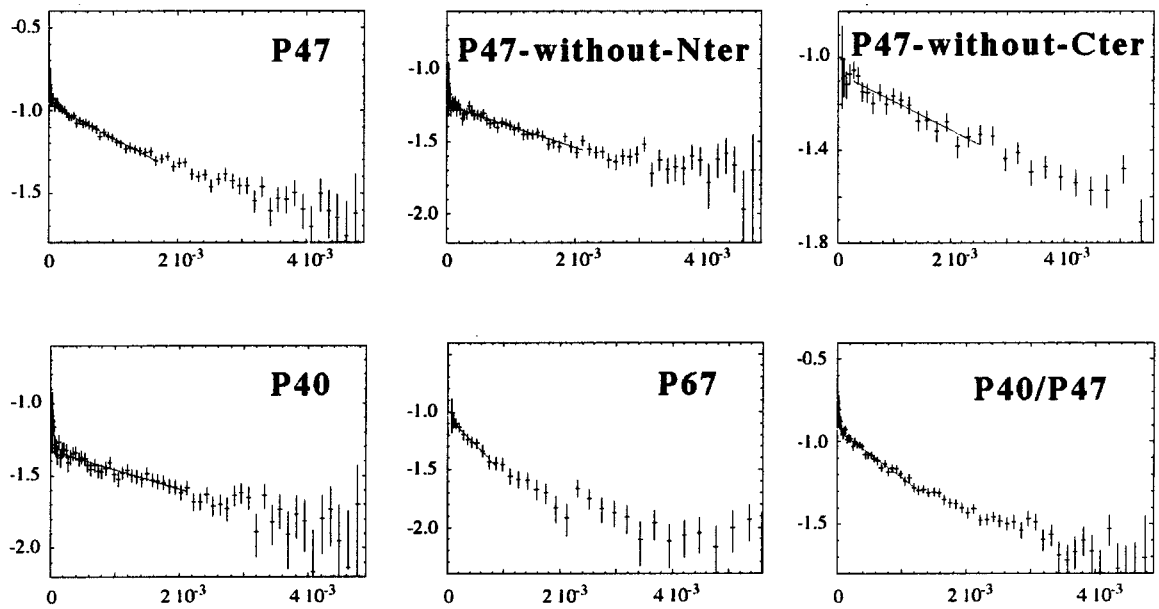

FIGURE 2: Neutron scattering Guinier plots. The plots represent ln $I(q)$, where $I(q)$ is the normalized scattered intensity, as a function of q^2 (Å^{-2}), where $q = 4\pi \sin\theta/\lambda$ and 2θ is the scattering angle. The radii of gyration, R_g, are obtained from linear fits at low q values ($R_g q < 1$, Guinier approximation).

Table 1: Parameters Determined from the Guinier Plot [$I(0)$, R_g, and Molecular Mass MW]

protein	concentration (mg/mL)	$I(0)$	R_g (Å)[a]	MW (Da)[b]	theoretical MW (Da)[c]
p47^{phox}-without-Cter	3.42	0.0885	28	45 375	43 367
p47^{phox}	4.10	0.110	36	47 044	47 316
p47^{phox}-without-Nter	3.12	0.058	32	32 596	29 117
p40^{phox}	2.17	0.048	29.5	39 949	40 500
p67^{phox}	1.16	0.0816	55	125 927	131 660
p40^{phox}−p47^{phox} complex	2.89	0.122	45	75 115 (74343)[d]	87 816

[a] The errors in R_g range from ±1 to ±2 Å. [b] The errors in MW are estimated to be 10%; they derive from the errors in $I(0)$ in the fit of the Guinier plot (a few percent) and errors in the concentration measurements. [c] Theoretical masses are calculated from the amino acid sequences. [d] The mass of the complex is estimated in two ways: (1) by using the concentrations of the proteins as determined from the absorbance measurements (MW in parentheses) and (2) by correcting these concentrations from the $I(0)$ values of the individual proteins considering the exact mass of the protein [$c = I(0)/kM$]. The second calculation possibly corrects for errors in the concentrations of individual proteins.

As p67^{phox} had a tendency to form insoluble clusters in bacterial extracts, it was expressed in insect cells. The C-terminal extension of p47^{phox} containing the proline rich motif is known to be essential for NADPH oxidase activation, most probably because it interacts with another cytosolic factor. To test this hypothesis, a number of constructs of p47^{phox} were used: the full-length p47^{phox}, p47^{phox} without the C-terminal extension (p47^{phox}-without-Cter), and p47^{phox} without the N-terminal extension restricted to the two SH3 domains and to the C-terminus (p47^{phox}-without-Nter) (Figure 1). Figure 2 shows the Guinier plots for all the individual cytosolic factors (p47^{phox}, p40^{phox}, and p67^{phox}), for a truncated form of p47^{phox}, and for the association of p47^{phox} with p40^{phox}. Table 1 summarizes the experimental conditions and the results of the analysis of the SANS experiments.

Molecular Masses. The comparison of the molecular masses of the three forms of p47^{phox} and of p40^{phox} experimentally determined with the theoretical masses calculated from the sequences indicates that the proteins are monomers. For p67^{phox}, the mass is consistent with a dimer, which was confirmed by gel filtration analysis. The poor solubility of some of the individual cytosolic factors is a severe limitation for studying protein−protein associations. Only results from experiments in which the individual proteins were prepared in monodispersed solutions were used to derive calculations (Figure 2 and Table 1). The equimolar mixing of p47^{phox} and p40^{phox} reveals the formation of a 1:1 complex. Comparison of the experimental and calculated $I(0)$ values shows that the $I(0)$ of the p40^{phox}−p47^{phox} complex is closer to that of a 1:1 complex than to that of isolated proteins in solution. When no complex is formed, $I(0)$ can be calculated from the relation

$$I(0) = k_1 c_1' M_1 + k_2 c_2' M_2$$

where c_1' and c_2' are the concentrations of proteins 1 and 2 in the final solution and k_1 and k_2 are derived from the amino acid sequences of proteins 1 and 2, respectively. Before the two protein solutions were mixed, the scattering intensity at zero angle for each protein is $I_1(0) = k_1 c_1 M_1$, where c_1 is the protein concentration before mixing the two protein solutions, c_1' is related to c_1 by the equation $c_1' = \upsilon_1 c_1/(\upsilon_1 + \upsilon_2)$, where υ_1 and υ_2 refer to the volumes of proteins 1 and 2, respectively. Therefore, $I(0)$ can be equal to $[\upsilon_1 I_1(0) + \upsilon_2 I_2(0)]/(\upsilon_1 + \upsilon_2)$. When a complex forms, $I(0)$ is calculated from the relation $I(0) = kcM$, where k and M are derived from the amino acid sequences of both proteins forming the complex and c is the experimental protein concentration. The calculated $I(0)$ values thus obtained are 0.072 and 0.143 for noncomplexed and complexed species, respectively. From the comparison of these values with the experimental $I(0)$, we estimate that 70% of the p47^{phox} molecules and p40^{phox} molecules in solution are associated in a complex. Because the masses of p40^{phox} and p47^{phox} are not so different, the mass obtained for the mixture does not exclude the possibility of the formation of homodimers.

SANS measurements indicated that p40^{phox} and p47^{phox}, assayed separately prior to the mixing, were in a monomeric state. A reorganization of either p40^{phox} or p47^{phox} in homodimers therefore appears to be improbable. Additional gel filtration experiments described in this paper confirm the formation of a p40^{phox}−p47^{phox} heterodimer.

Radii of Gyration. The radius of gyration of a particle reflects the distribution of scattering matter within the particle through the relationship $R_g^2 = \Sigma b_i r_i^2 / \Sigma b_i$, where b_i is the scattering length corrected for contribution of solvent of atom i and r_i is its position, and the sum is over all atoms in the particle. For a given mass, the minimum R_g that is possible is given by the equivalent sphere, and any deviations from sphericity increase R_g. We calculated radii of gyration of various proteins for which the atomic coordinates are known using the program described in ref *24* and found deviations of 20% (for globular proteins) to 50% (for elongated proteins) from the values which would be expected for a uniform sphere (data not shown). The radii of gyration, R_g, obtained in our experiments for the individual proteins and the complexes are shown in Table 1. Interestingly, p47^{phox}-without-Cter has a much smaller radius than p47^{phox}, 28 versus 36 Å, despite a modest decrease in molecular mass (less than 8%). In contrast, p47^{phox}-without-Nter has an R_g of 32 Å. The R_g of 29.5 Å for p40^{phox} deviates largely from a value that can be ascribed to a globular protein. Upon binding of p40^{phox} to p47^{phox}, the R_g value increases to 45 Å which suggests the formation of a very elongated complex. The R_g value for p67^{phox} also denotes an elongated form for the dimer.

Gel Filtration Analysis

To ascertain the formation of a heterodimer and to assess the role of the C-terminal polyPro motif of p47^{phox} in the association with p40^{phox}, gel filtration was performed on a mixture of p40^{phox} fused to thioredoxin (Trx-His-p40^{phox}) and a mixed solution of p47^{phox} and p47^{phox}-without-Cter as usually obtained prior to the last purification step of p47^{phox}. As shown in Figure 3a, Trx-His-p40^{phox} in fractions 17−19 coelutes with the full-length p47^{phox} in an elution volume corresponding to that of the p40^{phox}−p47^{phox} heterodimer. p47^{phox}-without-Cter started to be eluted in fraction 19 and was totally recovered in fractions 20 and 21. The proximity of the two peaks of elution was responsible for some minor cross contamination. Moreover, when a mixed solution of the MBP-SH3^{p40phox} fusion protein and p47^{phox}-without-Nter were loaded onto an amylose column, the p47^{phox}-without-Nter protein coeluted with the MBP-SH3^{p40phox}, using a maltose gradient. This illustrates the specific interaction between the SH3 domain of p40^{phox} and p47^{phox}. The eluted complex was then loaded onto a Superdex 200 gel filtration column. A 1:1 complex was again observed, well separated from an excess of MBP-SH3^{p40phox}, as assessed by migration on SDS−PAGE (Figure 3b). This was confirmed by comparison of the elution volume to elution volumes of gel filtration standards. These experiments indicate that C-terminal amino acids 355−390 of p47^{phox} are essential for the interaction with the SH3 domain of p40^{phox}. The control experiment with MBP alone in the presence of p47^{phox}-without-Nter revealed no complex formation.

The analysis of the oligomeric state of p67^{phox} by gel filtration on Superdex 200 shows that p67^{phox} is dimeric

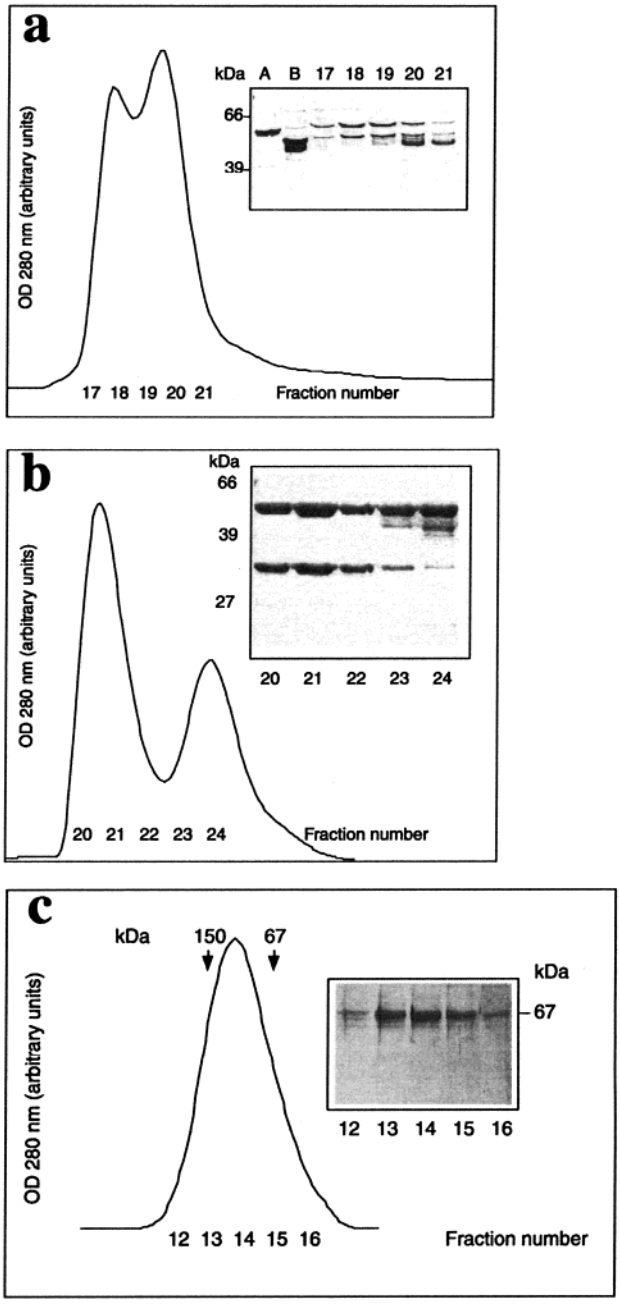

FIGURE 3: Gel filtration chromatograms and SDS−PAGE gels. (a) p47^{phox} (47 kDa) and p47^{phox}-without-Cter (43 kDa) mixed with Trx-His-p40^{phox} (52 kDa), (b) MBP-SH3^{p40phox} (52 kDa) mixed with p47^{phox}-without-Nter (33 kDa), and (c) p67^{phox}. The gel filtration columns were Superdex 200. Lanes A and B in panel a represent separately Trx-His-p40^{phox} and the mixture of p47^{phox} with p47^{phox}-without-Cter, respectively. In panel c, the positions of the calibration markers, IgG (150 kDa) and BSA (67 kDa), are indicated with arrows.

(Figure 3c). This is consistent with previous reports showing that p67^{phox} purified from bovine neutrophils was dimeric (*25*).

DISCUSSION

Interaction of p40^{phox} with p47^{phox} in Solution. The association of p40^{phox} with p47^{phox} or p67^{phox} is less well documented than that of p47^{phox} with p67^{phox}. The domains of p40^{phox} interacting with p47^{phox}, and also with p67^{phox}, were mapped using the two-hybrid system (*18*, *26*). The SH3

domain of $p40^{phox}$ interacts with the polyPro motif of $p47^{phox}$, whereas the C-terminus of $p40^{phox}$, later recognized as the PC motif (*9*) and not its SH3, interacts with $p67^{phox}$ in the inter-SH3 region. The role of $p40^{phox}$ in NADPH oxidase activation is still a matter of debate. Different hypotheses have been suggested. $p40^{phox}$ could act by stabilizing $p67^{phox}$ in the resting state of the cell, whereby it could downregulate the oxidase activity by competitive interaction between its SH3 domain and strategic components of the oxidase complex (*27*). Our SANS experiments show that $p40^{phox}$ binds to the full-length $p47^{phox}$ in solution in the absence of phosphorylation. This is confirmed by gel filtration experiments. Moreover, in the absence of its C-terminus, $p47^{phox}$ is unable to bind to $p40^{phox}$, and in contrast, in the absence of its N-terminus, $p47^{phox}$ is able to bind to the SH3 domain of $p40^{phox}$. Therefore, the interactions between $p40^{phox}$ and $p47^{phox}$ can essentially be ascribed to the SH3 domain of $p40^{phox}$ interacting with the polyPro motif of $p47^{phox}$.

Intramolecular Interactions in $p47^{phox}$. The NADPH oxidase is activated upon exposure of intact cells to appropriate stimuli, and under these conditions, oxidase activation is related to the phosphorylation of $p47^{phox}$ (*4*). In a reconstituted activation system (*17*, *28*), a similar effect is achieved by adding anionic amphiphiles such as SDS or arachidonic acid. It was postulated that phosphorylation or amphiphilic reagents act by disrupting intramolecular interactions in $p47^{phox}$. Earlier studies suggested that intramolecular interactions could occur between the polyPro motif and the N-terminal SH3 domain (*29*), resulting in a hairpin folding from residue 151 to residue 390, and activation was correlated with the opening of the hairpin. A more detailed analysis (*30*) demonstrated that the N-terminal SH3 of $p47^{phox}$ interacts with a sequence spanning residues 299−346, upstream of the polyPro motif and present in $p47^{phox}$-without-Cter. The radii of gyration observed here for $p47^{phox}$, $p47^{phox}$-without-Cter, and $p47^{phox}$-without-Nter suggest that all these molecules are elongated, $p47^{phox}$ and $p47^{phox}$-without-Nter being the most elongated. The N-terminal end of $p47^{phox}$ is globular as shown from the small difference in R_g between $p47^{phox}$ and $p47^{phox}$-without-Nter. The smaller value measured for $p47^{phox}$-without-Cter suggests an intramolecular interaction**,** which may be explained by interaction of the SH3 domain with residues 299−346. For the full-length $p47^{phox}$, intramolecular interactions are unlikely since the larger R_g value denotes a very elongated molecule. The role of amphiphiles or of $p47^{phox}$ phosphorylation during NADPH oxidase activation could therefore be to disrupt the $p40^{phox}$—$p47^{phox}$ complex rather than to break an intramolecular interaction in $p47^{phox}$.

ACKNOWLEDGMENT

We acknowledge M. Jaquinod for mass spectrometry measurements, C. Cohen-Addad, C. Ebel, and J. Gagnon for fruitful discussions, and I. Ayala for technical assistance. Neutron scattering experiments were carried out at the Institut Laue-Langevin.

REFERENCES

1. Babior, B. M. (1999) *Blood 93*, 1464−1476.
2. DeLeo, F. R., and Quinn, M. T. (1996) *J. Leukocyte Biol. 60*, 677−691.
3. El Benna, J., Faust, L.-R. P., Johnson, J. L., and Babior, B. M. (1996) *J. Biol. Chem. 271*, 6374−6378.
4. Park, J.-W., and Babior, B. M. (1997) *Biochemistry 36*, 7474−7480.
5. Fuchs, A., Bouin, A. P., Rabilloud, T., and Vignais, P. V. (1997) *Eur. J. Biochem. 249*, 531−539.
6. El Benna, J., Dang, P. M., Gaudry, M., Fay, M., Morel, F., Hakim, J., and Gougerot-Pocilado, M.-A. (1997) *J. Biol. Chem. 272*, 17204−17208.
7. Forbes, L. V., Truong, O., Wientjes, F. B., Moss, S. J., and Segal, A. W. (1999) *Biochem. J. 338*, 99−105.
8. Ponting, C. P. (1996) *Protein Sci. 5*, 2353−2357.
9. Nakamura, R., Sumimoto, H., Mizuki, K., Hata, K., Ago, T., Kitajima, S., Takeshige, K., Sakaki, Y., and Ito, T. (1998) *Eur. J. Biochem. 251*, 583−589.
10. Diekmann, D., Abo, A., Johnson, C., Segal, A., and Hall, A. (1994) *Science 265*, 531−533.
11. Han, C.-H., Freeman, J. L. R., Lee, T., Motalebi, S. A., and Lambeth, J. D. (1998) *J. Biol. Chem. 273*, 16663−16668.
12. Koga, H., Terasawa, H., Nunoi, H., Takeshige, K., Fuyuhiko, I., and Sumimoto, H. (1999) *J. Biol. Chem. 274*, 25051−25060.
13. Prigmore, E., Ahmed, S., Best, A., Kozma, R., Manser, E., Segal, A. W., and Lim, L. (1995) *J. Biol. Chem. 270*, 10717−10722.
14. Cohen, G. B., Ren, R., and Baltimore, D. (1995) *Cell 80*, 237−248.
15. Pawson, T. (1995) *Nature 373*, 573−580.
16. Grandvaux, N., Grizot, S., Vignais, P. V., and Dagher, M.-C. (1999) *J. Cell Sci. 112*, 503−513.
17. Fuchs, A., Dagher, M.-C., Jouan, A., and Vignais, P. V. (1994) *Eur. J. Biochem. 226*, 587−595.
18. Fuchs, A., Dagher, M.-C., and Vignais, P. V. (1995) *J. Biol. Chem. 270*, 5695−5697.
19. Ibel, K. (1976) *J. Appl. Crystallogr. 9*, 296−309.
20. Ghosh, R. E., Egelhaaf, S. U., and Rennie, A. R. (1998) A computing guide for small angle scattering experiments, Technical Report ILL98GH14T, Institut Laue-Langevin, Grenoble, France.
21. Jacrot, B., and Zaccai, G. (1981) *Biopolymers 20*, 2413−2426.
22. Jacrot, B. (1976) *Rep. Prog. Phys. 39*, 911−953.
23. Moore, A. T., and Stein, W. H. (1963) in *Methods in Enzymology* (Colowick, S. P., and Kaplan, N. O., Eds.) Vol. 6, pp 819−830, Academic, New York.
24. Svergun, D. I., Richard, S., Koch, M. H., Sayers, Z., Kuprin, S., and Zaccai, G. (1998) *Proc. Natl. Acad. Sci. U.S.A. 95*, 2267−2272.
25. Pilloud-Dagher, M.-C., and Vignais, P. V. (1991) *Biochemistry 30*, 2753−2760.
26. Fuchs, A., Dagher, M. C., Faure, J., and Vignais, P. V. (1996) *Biochim. Biophys. Acta 1312*, 39−47.
27. Sathyamoorthy, M., De Mendez, I., Adams, A. G., and Leto, T. L. (1997) *J. Biol. Chem. 272*, 9141−9146.
28. Abo, A., and Pick, E. (1991) *J. Biol. Chem. 266*, 23577−23585.
29. Leto, T. L., Adams, A. G., and de Mendez, I. (1994) *Proc. Natl. Acad. Sci. U.S.A. 91*, 10650−10654.
30. Hata, K., Ito, K., Takeshige, K., and Sumimoto, H. (1998) *J. Biol. Chem. 273*, 4232−4236.

BI0028439